RESEARCH ARTICLE

For reprint orders, please contact: reprints@futuremedicine.com

Future MICROBIOLOGY

Evaluation of antibacterial and antibiofilm mechanisms by usnic acid against methicillin-resistant *Staphylococcus aureus*

Arianna Pompilio[‡,1,2], Antonella Riviello[‡,1,2,3], Valentina Crocetta[1,2], Fabrizio Di Giuseppe[1,2,3], Stefano Pomponio[1,2], Marilisa Sulpizio[1,2,3], Carmine Di Ilio[1,2,3], Stefania Angelucci[1,2,3], Luana Barone[4], Andrea Di Giulio[4] & Giovanni Di Bonaventura[*,1,2]

Aim: To evaluate the antibacterial and antibiofilm mechanisms of usnic acid (USN) against methicillin-resistant *Staphylococcus aureus* from cystic fibrosis patients. **Materials & methods**: The effects exerted by USN at subinhibitory concentrations on *S. aureus* Sa3 strain was evaluated by proteomic, real-time PCR and electron microscopy analyses. **Results & conclusion:** Proteomic analysis showed that USN caused damage in peptidoglycan synthesis, as confirmed by microscopy. Real-time PCR analysis showed that antibiofilm activity of USN is mainly due to impaired adhesion to the host matrix binding proteins, and decreasing lipase and thermonuclease expression. Our data show that USN exerts anti-staphylococcal effects through multitarget inhibitory effects, thus confirming the rationale for considering it 'lead compound' for the treatment of cystic fibrosis infections.

First draft submitted: 9 March 2016; Accepted for publication: 7 July 2016; Published online: 16 September 2016

KEYWORDS
- biofilm
- *Staphylococcus aureus*
- usnic acid

The most common cause of death in cystic fibrosis (CF) patients is respiratory failure secondary to pulmonary infection. *Pseudomonas aeruginosa* and *Burkholderia cepacia* complex are the pathogens most commonly associated with a shortened life span, although there has recently been an increase in the prevalence of several potentially pathogenic microorganisms in CF.

Methicillin-resistant *Staphylococcus aureus* (MRSA) is one such important emerging pathogen. Patients with CF are at particular risk for pulmonary colonization of MRSA because of two main factors: their difficulty in clearing mucus and their frequent hospital visits, which can increase exposure to MRSA [1–3]. *S. aureus* multiplies and persists in the airways of CF patients for months or even years despite appropriate anti-staphylococcal therapy [4,5]. Particularly, hospital-acquired MRSA isolates that are usually associated with SCC*mec* types I, II and III, tend to be resistant to all antimicrobials with the exception of glycopeptides.

Despite the increasing prevalence of MRSA in CF patients, its clinical significance remains unclear. Chronic pulmonary infection with MRSA is thought to confer CF patients a worse overall clinical outcome and, in particular, result in an increased rate of lung function decline, as measured by FEV_1 [3]. In contrast with this finding, another study using data from the Epidemiologic Study of Cystic Fibrosis showed that patients with MRSA had increased decline in lung function prior to MRSA

[1]Department of Medical, Oral & Biotechnological Sciences, 'G d'Annunzio' University of Chieti-Pescara, Via Vestini 31, Chieti, Italy
[2]Aging Research Center and Translational Medicine, 'G d'Annunzio' University of Chieti-Pescara, Via L Polacchi 13, Chieti, Italy
[3]Stem TeCh Group, Via L Polacchi 13, Chieti, Italy
[4]Department of Science, LIME, University Roma Tre, Viale G Marconi 446, Rome, Italy
*Author for correspondence: Tel.: +39 087 1355 4812; Fax: +39 087 1355 4822; gdibonaventura@unich.it
‡Authors contributed equally

Future Medicine part of fsg

acquisition therefore concluding that MRSA did not influence lung function decline [6].

In addition to methicillin resistance, other adaptive strategies are adopted by *S. aureus* to survive in CF lung, such as the formation of biofilms and the switch to small-colony variants, therefore making the action of antimicrobial agents and pathogen eradication difficult [7–9].

The relevant morbidity and mortality associated with *S. aureus* infection and the increased antibiotic resistance demand the development of new antimicrobial strategies.

Natural products with diverse bioactivities and structures are an important source of novel chemicals with pharmaceutical potentials. Lichens, symbiotic organisms between a fungal (mycobiont) and algal and/or cianobacterial (phytobiont) partner, are commonly found worldwide. This symbiotic relationship is undeniably successful for lichens that can survive a variety of harsh environmental conditions and are inherently resistant to microbial infections. Their intrinsic resistance is mainly due to the production of a large number of compounds that typically arise from the secondary metabolism of the fungal component. Chemotaxonomic studies have shown that most lichen secondary metabolites belong to the chemical classes of depsides, depsidones and dibenzofurans [10].

Of the hundreds of known secondary lichen metabolites, the benzofuran derivative usnic acid (USN), commonly found in the genus *Usnea*, is the most studied. Lichens belonging to USN producers have been extensively used for centuries in folklorist medicine in the treatment of pulmonary tuberculosis, pain relief, fever control, wounds, mycoses, sore throat, toothache and several skin infections [11,12]. In fact, USN has shown a variety of biological activities, including antimicrobial activity against a number of bacterial and fungal pathogens, both tested as planktonic and sessile (biofilm) lifestyle [13–16]. Toxicity in USN must be addressed due to some adverse reports relating its use as a slimming agent and dietary supplement [17]. Hepatotoxicity has been deeply investigated, although USN has been reported to induce toxicity in other normal and malignant cell types [18]. However, adsorbing USN onto different carriers (i.e., polymers, magnetic nanoparticles) reduces toxicity [19,20] as well as affects biofilm development and facilitates eradication of preformed biofilms [19,21–23].

Recently, our group found that USN shows relevant activity against both planktonic and biofilm lifestyles of *S. aureus* strains isolated from CF patients [24], therefore warranting further *in vitro* and *in vivo* studies to evaluate the 'real' potential of this lichen metabolite in the management of lung infections in CF patients. Although the antibiotic activity of USN is nowadays universally recognized, little or nothing is known about its mechanism of action.

In the present work, for the first time, proteomic analysis was performed to investigate the effects caused by the exposure to USN at subinhibitory concentration on protein expression of an MRSA strain isolated from a CF patient. The morphological and ultrastructural changes induced by USN in staphylococcal cells were further elucidated using both transmission and scanning electron microscopy. Finally, the effects of USN at subinhibitory concentrations on virulence gene expression by *S. aureus* were also investigated.

Materials & methods

• Bacterial strain & growth conditions

Staphylococcus aureus Sa3 strain was isolated from the airways of a chronically infected patient diagnosed with CF (genotype ΔF508/ΔF508) attending 'Bambino Gesù' Children Hospital of Rome, Italy. Identification at species level was carried out by conventional biochemical tests (API® Staph System; BioMérieux, Marcy-L'Etoile, France). Resistance to methicillin was evaluated with 30-µg cefoxitin disks and confirmed by a duplex PCR assay with primers targeting *nuc* and *mecA* genes, respectively [25]. Strain was stored at -80°C (Microbank®; Biolife Italiana S.r.l., Milan, Italy) until use when it was grown overnight at 37°C in Trypticase Soy broth (TSB; Oxoid S.p.A.; Garbagnate M.se, Italy), then plated twice on Mueller-Hinton Agar (MHA; Oxoid S.p.A.) to check for purity and to restore the original phenotype.

All assays were carried out by using a standardized bacterial inoculum. Briefly, some colonies grown overnight on MHA were resuspended in sterile NaCl to an OD_{550} of 1.2 (corresponding to 1–3 × 10^8 CFU/ml), then diluted 1:1000 in cation-adjusted Mueller–Hinton broth (CAMHB; Becton, Dickinson and Company; Milan, Italy; pH 7.2–7.4).

• Usnic acid

Usnic acid powder (Sigma-Aldrich; Milan, Italy) was used to prepare a 2 mg/ml stock solution in dimethyl sulfoxide (DMSO; Sigma-Aldrich)

and then diluted with sterile CAMHB to obtain desired concentrations. The final DMSO concentration (≤ 3%) did not affect the viability of the strain tested (data not shown).

• Minimum inhibitory concentration determination

Minimum inhibitory concentration (MIC) of USN for *S. aureus* Sa3 strain was 64 µg/ml, as assessed in triplicate using the microdilution method, according to the Clinical and Laboratory Standards Institute [26].

• Exposure to USN

The standardized inoculum was exposed to USN (for 24 h at 37°C) under static conditions, at desired concentrations: 1/64 × MIC, for proteomic studies because it was the highest subinhibitory concentration showing no effects on *S. aureus* Sa3 growth; 1/256×, 1/128× and 1/64 × MIC for gene expression analysis so as to evaluate if the effects were dose-dependent; and 1×, 1/8× and 1/64 × MIC for microscopic analysis so as to assess the continuum of ultrastructural effects from the inhibitory concentration (hypothetical max effect) toward the 'target' concentration of 1/64 × MIC. A bacterial suspension not exposed to USN was prepared as control (CTRL) for comparative purposes. The rationale for selecting USN concentrations was based on the evidence that USN did not affect bacterial growth at 1/64 × MIC (data not shown).

• Protein preparation & 2DE analysis

At the end of exposure to USN, bacterial cells were prepared according to previous studies, with minor modification, to obtain membrane fraction [27,28]. Each sample was electrophoretically run three times as three technical and two biological replicates. Protein concentration was measured using Better Bradford® (Pierce, IL, USA) and a total amount of 150 µg (for the analytical gels) and 500 µg (for preparative gels) were mixed with rehydration solution (DeStreak™ Rehydration Solution, GE Healthcare, Uppsala, Sweden), and both were applied to isoelectric focusing using IPG strip nonlinear pH 4–7, 24 cm (GE Healthcare) on Ettan™ IPGphor™ III System (GE Healthcare). The second dimension SDS-PAGE was performed on 9–16% SDS-polyacrylamide gels according to procedures previously described by Sulpizio *et al.* [29].

After staining, gels were scanned at 600 dpi with LabScan 5.0 (GE Healthcare) and, in order to create a reference gel representative of all analyzed conditions, three different gel runs for each group type (time zero, sedentary and trained) samples were performed and then subjected to image analysis with ImageMaster 2D Platinum 6.0 software (GE Healthcare). A reference gel was created from a representative gel combining all spots common to the various analyzed gels. The reference gel was then used to determine the presence and difference in protein expression among gels. Background subtraction was performed and the intensity volume of each spot was normalized with total intensity volume (summing the intensity volumes obtained from all spots within the same 2D gel). All the quantitative data are reported as mean ± standard error of the mean (SEM). The Intensity volumes of individual spots were matched across the different gels and then compared among groups by multiple comparisons using one-way analysis of variance. Differently expressed ($p < 0.001$) protein spots underwent in-gel tryptic digestion and identification by mass spectrometry (MS).

• Protein digestion & MALDI-TOF/TOF-MS analysis

Protein spots were excised from 2D gels and analyzed using peptide mass finger printing (PMF) approach with a MALDI-TOF/TOF spectrometer. Following protein spot digestion in 50 mM NH_4HCO_3 containing trypsin and incubated overnight at 37°C [25], the peptide extract was applied to aC18ZipTip (Millipore, CA, USA), rinsed with a 0.1% TFA and eluted directly on the MALDI target with 0.5 µl of a saturated α-cyano-4-hydroxycinnamic acid (1:1 = ACN: 0.1% TFA) solution.

Tryptic digests were analyzed by Autoflex™ Speed mass spectrometer (Bruker Daltonics, Bremen, Germany) equipped with a Nd:YAG laser (355 nm; 1000 Hz) operated by FlexControl v3.3 and equipped with a 355-nm nitrogen laser. All spectra were obtained with the delayed extraction technology in positive reflectron mode and averaged from 100 laser shots to improve the S/N ratio. External high precision calibration was performed using a peptide mixture containing bradykinin (fragment 1–7) 757.39 *m/z*, angiotensin II 1046.54 *m/z*, ACTH (fragment 18–39) 2465.19 *m/z*, Glu fibrinopeptide B 1571.57 *m/z* and renin substrate tetradecapeptide porcine 1760.02 *m/z*. Samples analyzed by PMF were additionally analyzed using LIFT MS/MS from the same target. The

most abundant ions per sample were chosen for MS/MS analysis. Analyses were performed in positive LIFT reflectron mode. Precursor ion selector range was 0.65% of parent ion mass. The voltage parameters were set at IS1 6 kV, IS2 5.3 kV, lens 3.00 kV, reflector 1 27.0 kV, reflector 2 11.45 kV, LIFT1 19 kV and LIFT 2 4.40 kV.

• Database MS/MS searching

Following MS acquisition, each spectrum was submitted to PMF to search the mouse NCBIn protein database using a Mascot search engine, which compares the experimentally determined tryptic peptide masses with theoretical peptide masses calculated for protein from these databases. Search parameters are as follows: search type, peptide mass fingerprint enzyme, trypsin; fixed modification, carbamidomethylation (Cys); variable modifications, oxidation of methionine; mass values, monoisotopic; ion charge state was set to +1; maximum miscleavages was set to 1; mass tolerance of 100 ppm for PMF and 0.6–0.8 Da for MS/MS. After automated assessment of the search results, the samples were automatically submitted to LIFT TOF/TOF acquisition for validation of data analysis from PMF. A maximum of four precursor ions per sample were chosen for MS/MS analysis. Protein database searches, through Mascot, using combined PMF and MS/MS datasets were performed via BioTools 3.2 (Bruker Daltonics) connected to the Mascot search engine used for SwissProt database (SwissProt_2012_03.fasta) search of datasets. The match with the lowest probability, that is, the highest score is reported as the best match. Identity threshold is typically a score of about 70 for PMF and 30–40 for MS/MS search. Whether the best match will be significant depends on data quality and the size of the database. Ideally, the correct match is the best and significant match.

• Bioinformatic analysis of proteomic data

Identified proteins were further analyzed using the STRING software [30], chosen as the source for protein–protein interactions, to statistically evaluate the functions and pathways most strongly associated with the protein list. Protein ontology classification was performed by importing proteins into the protein analysis through gene ontology (GO) classification system [31]. Proteins were grouped according to their associated biological processes and molecular functions.

• Gene expression assay

The effect of USN at sub-MICs on the transcription levels of 11 virulence factors of *S. aureus* Sa3 was assessed by RT-PCR **(Table 1)**. *S. aureus* Sa3 was cultured, both in the presence and absence of USN (at 0.25, 0.5 and 1 µg/ml, corresponding at 1/256×, 1/128× and 1/64 × MIC, respectively) as described above. Following 24-h incubation at 37°C, samples were washed by centrifugation and then harvested in QIAzol (Qiagen©) with lysozyme 10 mg/ml. RNA was then extracted by phenol-chloroform technique, treated with DNase I (TURBO DNA-free™; Applied Biosystems, Monza, Italy), and checked for purity by NanoDrop-200 spectrophotometer (Thermo Scientific). cDNA strand was synthesized using a High Capacity cDNA reverse transcription kit (Applied Biosystems) per manufacturer protocol. All experiments were performed by using 450 ng of RNA converted in cDNA. Gene expression was evaluated using a SYBRgreen (Applied Biosystems) RT-PCR assay. The primers' specificity was assessed both *in silico* with BLAST and by PCR endpoint in the same RT-PCR conditions. The ΔΔCt method was used to determine relative gene expression of each gene [32], both in the presence or absence of USN, normalized to expression of the housekeeping gene *gyrB*. Differences in gene expression levels were evaluated by a paired Student's *t*-test, considering a $p < 0.05$ as statistically significant.

• Electron microscopic analyses

The effects of USN on staphylococcal morphology were assessed through scanning (SEM) and transmission (TEM) electron microscopy [36,37].

TEM

Bacteria were cultured overnight in grown medium in the absence or presence of USN at different concentrations – corresponding to 1×, 1/8× and 1/64 × MIC – and were then harvested by centrifugation at 10,000 × *g* for 5 min. The cells were washed twice, resuspended in phosphate buffered saline (Sigma-Aldrich) and fixed with 2.5% glutaraldehyde in 0.1 M cacodylate buffer, pH 7.4, 1 h at 4°C. After incubation, the cells were recovered by centrifugation at 10,000 × *g* for 5 min. After being washed twice in cacodylate buffer, the pellets were postfixed with 1% osmium tetraoxide (OsO_4) in 0.2 M cacodylate buffer for 1 h at

Table 1. Quantitative PCR primers used in this study to assess the effects of usnic acid at sub-minimum inhibitory concentrations on the expression levels of selected virulence factors by *S. aureus* Sa3 strain.

Primer sequence, 5′–3′	Primer ID	Target gene	Gene function	Ref.
GAGGTAAAGCCAACGCACTC	*icaA*-F	*icaA*	Intercellular adhesin	[33]
CCTGTAACCGCACCAAGTTT	*icaA*-R			
ATACCGGCGACTGGGTTTAT	*icaB*-F	*icaB*	Intercellular adhesin	[33]
TTGCAAATCGTGGGTATGTGT	*icaB*-R			
CTTGGGTATTTGCACGCATT	*icaC*-F	*icaC*	Intercellular adhesin	[33]
GCAATATCATGCCGACACCT	*icaC*-R			
ACCCAACGCTAAAATCATCG	*icaD*-F	*icaD*	Intercellular adhesin	[33]
GCGAAAATGCCCATAGTTTC	*icaD*-R			
AAATTGGGAGCAGCATCAAGT	*fnbA*-F	*fnbA*	Receptor for fibronectin	[33]
GCAGTCGAATTCCCATTTTC	*fnbA*-R			
CGTCAACAGCAGATGCGAGCG	*fib*-F	*fib*	Receptor for fibrinogen	[33]
TGCATCAGTTTTCGCTGCTGGTTT	*fib*-R			
GGTGCAGCTGGTGCAATGGGTGT	*ebps*-F	*ebps*	Receptor for elastin	[33]
GCTGCGCCTCCAGCCAAACCT	*ebps*-R			
TGCCGTAGGTGACGAAGGTGGTT	*eno*-F	*eno*	Receptor for laminin	[33]
GCACCGTGTTCGCCTTCGAACT	*eno*-R			
TGATAATCCTTATGAGGTGCTT	*agrA*-F	*agrA*	Quorum-sensing system	[34]
CACTGTGACTCGTAACGAAAA	*agrA*-R			
TCGCTTGCTATGATTGTGGTAGCC	*nuc*-F	*nuc*	Thermonuclease	[35]
TACAGGCGTATTCGGTTTCACCGT	*nuc*-R			
GTTGGCTCAATGGGGTCTAA	*geh*-F	*geh*	Lipase	[35]
CTCACGCGTCAGATCGTAAA	*geh*-R			

room temperature. The samples were dehydrated with graded ethanol solutions (70% ethanol 10 min, 80% ethanol 10 min, 95% ethanol 10 min and twice in 100% ethanol 15 min), embedded in Epon 812 resin and left to polymerize for 3 days.

Each sample was sectioned by a Reichert Ultracut S ultramicrotome. Ultrathin sections were briefly contrasted with uranyl acetate and observed using a Philips CM120 TEM equipped with a Philips Megaview III camera at the Interdepartmental Laboratory of Electron Microscopy (L.I.M.E., Roma Tre University, Rome, Italy).

SEM

For high resolution SEM images, the specimens were fixed as described for TEM, postfixed with osmium tetraoxide, dehydrated to 100% ethanol through a graded ethanol series, dried by hexamethyldisilazane (allowed to dry for 1 h), mounted on aluminum stubs with adhesive carbon disks, gold coated in an Emitech K550 unit and finally examined by using the field emission SEM column of the DualBeam FIB/SEM Helios Nanolab (FEI Company, Eindhoven, The Netherlands) at the L.I.M.E., with secondary electrons and an operating voltage of 5 kV. Electronic images were taken by AnalySys 2.0 software and composed in Adobe Photoshop CC format.

• Propidium iodide uptake assay

The effect of USN on *S. aureus* Sa3 membrane permeability was studied by measuring propidium iodide (PI) uptake by bacterial cells. Cell suspensions, prepared as described above, were aliquoted in each well of a microtiter plate (100 µl/well) in the presence of USN at 1/64×, 1/128× and 1/256 × MIC. Control samples consisted of bacterial suspension only. After 24-h treatment, PI (100 µl at 60 µM) was added to each sample and incubated at room temperature for 15 min in the dark. Fluorescence was measured at excitation and emission wavelengths of 485 and 630 nm, respectively, using a SINERGY™ H1 microplate reader (BioTek; Winooski, VT, USA). Differences in PI uptake levels were evaluated by analysis of variance followed by Tukey's multiple comparison post-test, considering a $p < 0.05$ as statistically significant.

Results

• Detection & analysis of *S. aureus* proteins differentially expressed following treatment with USN

To investigate the changes in *S. aureus* protein expression induced by USN, *S. aureus* Sa3 cultures were grown both in the absence and in the presence of USN at 1/64 × MIC and underwent 2DE analysis. **Figure 1** shows representative gels obtained for USN and CTRL samples. In both samples most of the protein spots were observed in the acidic range. Approximately 1.230 ± 99 and 1.108 ± 60 protein spots were observed on the 2DE-gel from surfacomes of CTRL and USN samples, respectively. A total of 1.003 ± 68 proteins were shared by both CTRL and USN samples, accounting for 81% of similarity. Twenty-six protein spots were identified to be differentially expressed ($p < 0.001$) on the 2DE maps of the two groups: 13 proteins were measured at increased levels compared with untreated cells, while 13 proteins were decreased **(Figure 2A)**. It is worth noting that five additional protein spots appeared only following exposure to USN **(Figure 2B)**.

Heuristic clustering analysis performed on all samples (three gels for four batches examined in both USN and CTRL samples) correctly identified two different phenotypes, USN and CTRL samples. On the right side of each panel the results from the evaluation of interclass variability are shown. The evaluation focused on those proteins that differed significantly ($p < 0.001$). For both phenotypes we used a magnification of 2D image showing the spot location and histogram to indicate the relative spot volume **(Figure 3)**.

The protein spots showing statistically significant fold change in normalized spot volume between USN and CTRL samples were excised, and digested for MS analyses. Information reporting differentially expressed protein spots – such as protein spot number, protein annotation and functional category (NCBI database) – are listed in **Table 2**.

The five proteins that were newly expressed following exposure to USN were identified as: three isoforms of acyl esterase, an haloacid dehalogenase (HAD) family hydrolase and the uncharacterized UPF0355 protein **(Table 3 & Figure 2)**.

• Functional analysis

Gene ontology functional analysis was carried out and results are shown in **Figure 4**. USN proteome was characterized by an increase of metabolic proteins (42 vs 40%, for USN and CTRL samples, respectively), and of those involved in protein synthesis and degradation processes (17 vs 15%, for USN and CTRL samples, respectively). A reduction was observed for proteins involved in cell cycle (8 vs 9%, for USN and CTRL samples, respectively), cell response

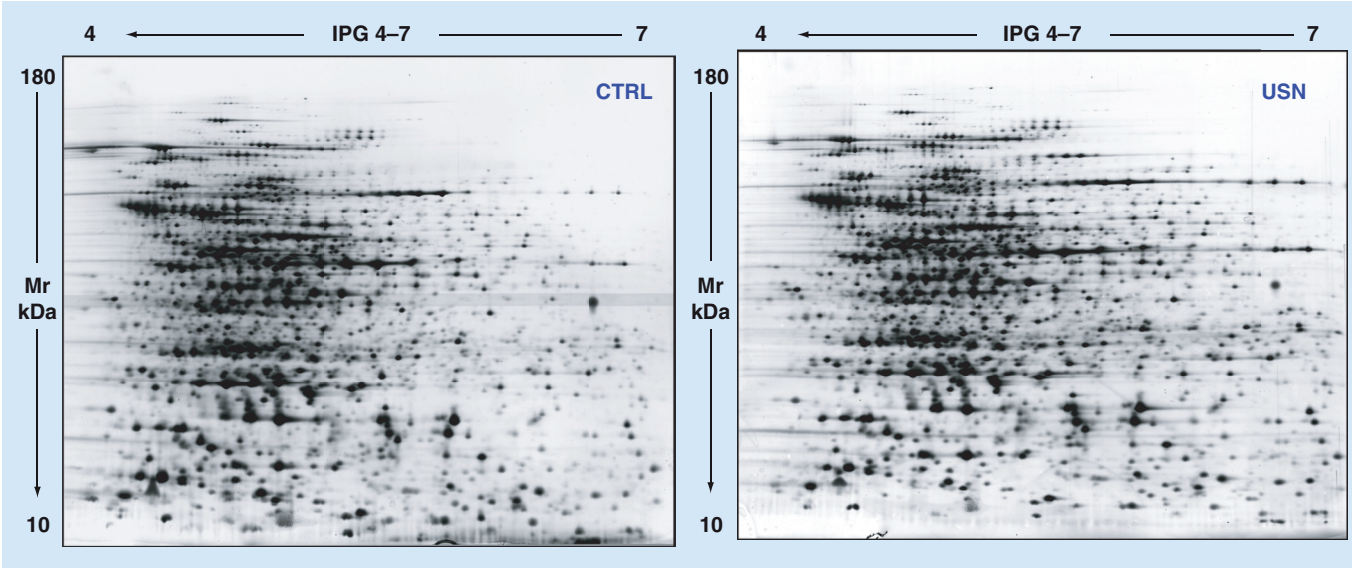

Figure 1. Representative 2DE maps of *Staphylococcus aureus* SA3 cultured without control or with usnic acid at 1 µg/ml (corresponding at 1/64 × minimum inhibitory concentration) for 24 h. Comparative analysis revealed at least 1.230 ± 99 and 1.108 ± 60 protein spots for CTRL and USN samples, respectively. One-hundred micrograms were loaded on IPG strip 4–7, 24 cm on 9–16% gradient gel.
CTRL: Control; USN: Usnic acid.

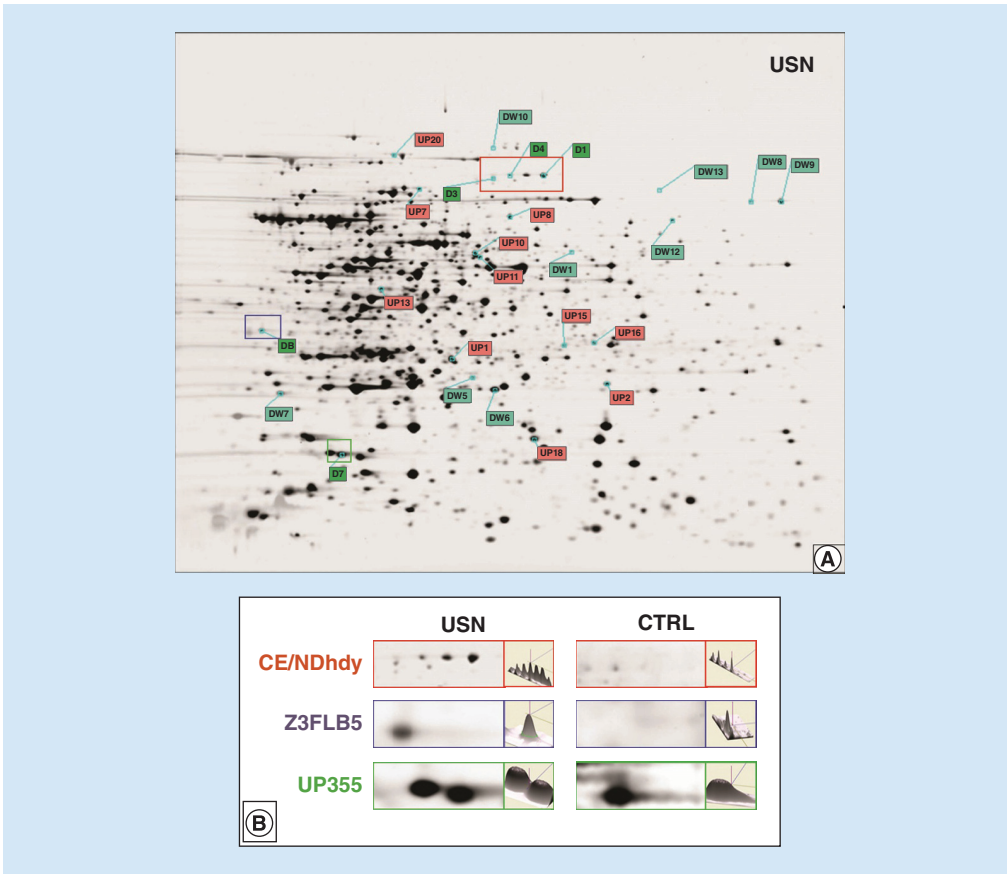

Figure 2. Identification of proteins differently expressed by *Staphylococcus aureus* SA3 after exposure to usnic acid at 1 µg/ml (corresponding at 1/64 × minimum inhibitory concentration) for 24 h.(A) 2D map of usnic acid-exposed sample: 26 proteins, resulted over- (red label) or under-regulated (green label), were unequivocally assigned. Representative different protein spots for expression level are shown. **(B)** Magnification of USN-related newly protein: CE/NDhdy (D1, D3, D7), Z3FLB5 (DB) and UP355 (D7) spots with its 3D view.
CTRL: Control; USN: Usnic acid.

to stress (19 vs 21%, for USN and CTRL samples, respectively) and nucleotide metabolism (13 vs 15%, for USN and CTRL samples, respectively). However, all of these differences resulted not to be statistically significant. No changes were observed for proteins involved in cell signaling (1%).

• Interactome

All changes in protein expression level, observed in USN samples compared with CTRL ones, were analyzed using STRING software (version 9.05), obtaining two protein interaction networks (PINs), one for each USN and CTRL samples, as shown in **Figure 5**. PINs allowed us to evidence possible functional associations among proteins differentially and specifically expressed in USN samples **(Figure 5B)**. Seven interesting functional pathways were identified in USN samples **(Figure 5)**. In particular, pathway 1 is composed of protein regulators of fatty-acid biosynthesis, acyl carrier proteins as Acyl-CoA reductase (FABG), an USN-related downregulated enzyme showing a strong functional interaction with fabF, fabH and fabI, hub proteins related to a large number of other forms favoring the fatty-acid chain elongation process. Pathway 2 related to hexosamine metabolism includes glucosamine-6-phosphate isomerase (NAGB) and glutamine-fructose-6-phosphate aminotransferase (GLMS), two very active enzymes in the regulation of biosynthetic processes. This pathway is strongly connected to pathways 3 and 5, including proteins involved in the pholate's biosynthesis and metabolism, respectively (GLYA, FOLD). Finally, pathway 7 showed a

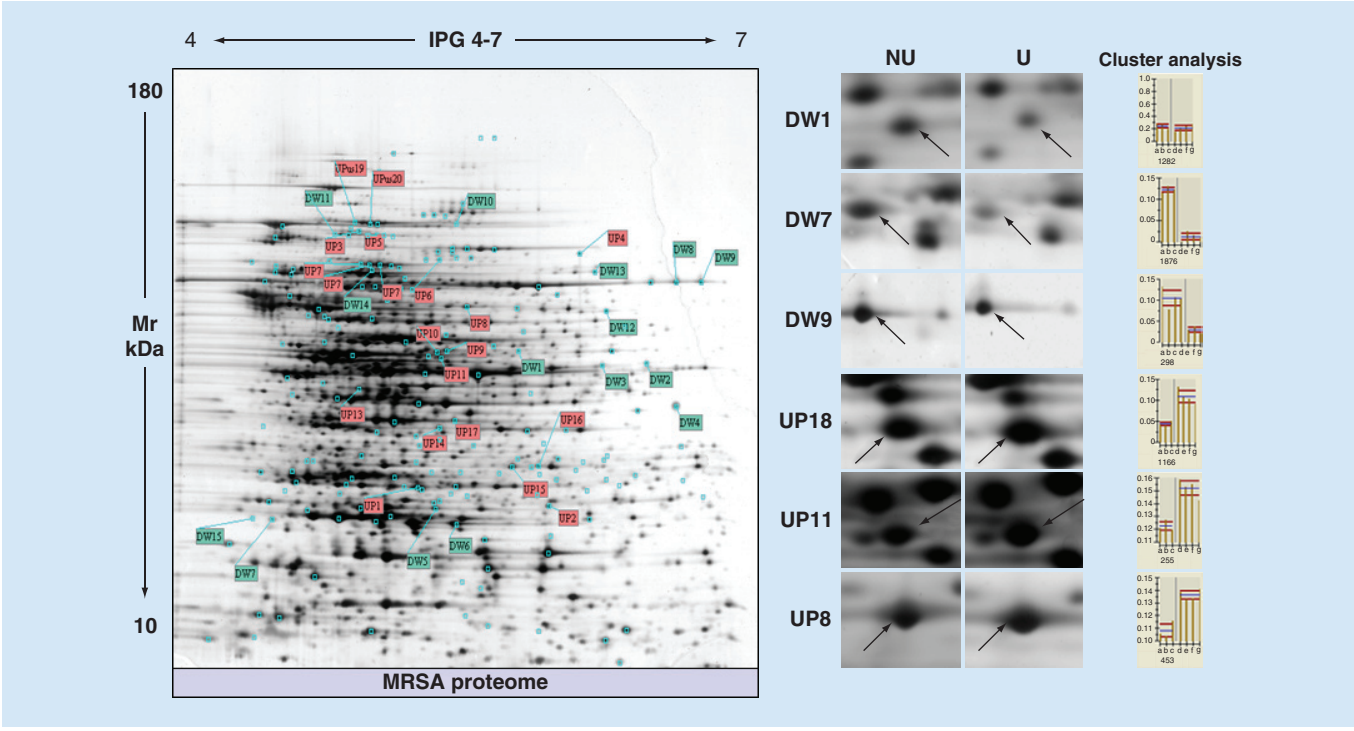

Figure 3. Usnic acid-related differentially expressed proteins. Master gel of *S. aureus* SA3 proteome quantitative changes, obtained following exposure to usnic acid, is shown. Some MS-assigned proteins are labeled with the abbreviation on 2D map. On the right, the results from heuristic cluster analysis on those proteins that differ significantly ($p < 0.001$) are reported. Each phenotype (usnic acid and control samples) underwent 2D image magnification showing protein spot location and histogram to measure the expression level. On the x-axis, each letter indicates a single gel (from three biological replicates for each condition). The y-axis indicates the relative volume of the spot.
CTRL: Control; DW, Downregulated protein; UP, Upregulated protein; USN: Usnic acid.

strong functional association between PCKA and MQO2, both important for oxidative stress.

• Effect of USN on *S. aureus* virulence expression

We employed RT-PCR to investigate the relative expression of 11 genes encoding virulence factors in *S. aureus* Sa3 strain following exposure to USN at sub-MICs **(Figure 6)**. USN significantly modulated the expression of most of the genes examined. Particularly, the expression of those codifying for lipase (*geh*), thermonuclease (*nuc*) and the receptors for laminin (*eno*) and elastin (*ebps*) was markedly repressed by *S. aureus* Sa3 in the presence of USN, regardless of tested concentration and in a dose-independent manner.

Particularly, when cultured in the presence of USN at 1/64 × MIC, the transcriptional levels of *geh*, *nuc*, *eno* and *ebps* decreased by 9.5-, 11.5-, 3.9- and 15.8-fold, respectively.

On the contrary, the effect exerted on the receptor for fibronectin (*fnbA*), quorum-sensing (*agrA*) and intercellular adhesin (*icaB*, icaC and *icaD*) genes was dependent on the tested concentrations: USN at 1/256 × MIC caused hyperexpression, with the exception of *icaD*, while all genes were downexpressed in the presence of USN at a concentration of 1/128 × MIC; USN significantly reduced *fnbA* expression (decreased by 2.0-fold) only at 1/64 × MIC. A trend toward hyperexpression was also observed for *icaA* and *fib*, although differences did not reach statistical significance, probably due to the high variability as suggested by SD values.

• Effects of USN on *S. aureus* cell morphology & ultrastructure

To elucidate the physiological effects of USN against *S. aureus*, SEM and TEM analyses were performed and representative micrographs are shown in **Figure 7 & Figure 8**, respectively.

The electron microscopy analysis showed that USN strongly compromised cell structure, causing death in a dose-dependent manner.

Table 2. Proteins differentially expressed in *Staphylococcus aureus* Sa3 strain after exposure to usnic acid.

Label	Abbreviated name	Description name	pI theo	Mw theo	Score[†]	Swiss Prot/NCBI AC[‡]	Gene name	Molecular function	Biological process	Fold-change variation[§]	MS/MS[¶]
UP1	SCDA	Iron-sulfur cluster repair protein ScdA	5.01	25,640	117	Q2FK11	*scdA*	Metal ion binding	Protein repair_response to oxidative stress	+1.4	2
UP2	DEF	Peptide deformylase	5.68	20,604	118	Q5HGZ3	*def*	Iron ion binding_peptide deformylase activity	Translation	+1.6	2
UP7	GUAA	GMP synthase (glutamine-hydrolyzing)	5.03	58,465	62	Q6GC81	*guaA*	ATP binding_GMP synthase (glutamine-hydrolyzing) activity_pyrophosphatase activity_transferase activity	GMP biosynthetic process_glutamine metabolic process_trna processing	+1.1	–
UP8	CDR	Coenzyme A disulfide reductase	5.28	49,374	103	A7 × 0I7	*CDR*	CoA-disulfide reductase activity_NADP binding_ flavin adenine dinucleotide binding_protein disulfide isomerase activity	Cell redox homeostasis_ protein folding	+1.3	–
UP10	T1Y5V9	Putative NADH-dependent flavin oxidoreductase yqig	5.24	42,054	81	T1Y5V9	*SAKOR_00316*	FMN binding_ oxidoreductase activity	Oxidation–reduction process	+1.3	–
UP13	LACC	Tagatose-6-phosphate kinase	4.92	34,045	51	A7 × 575	*lacC*	ATP binding_tagatose-6-phosphate kinase activity	D-tagatose 6-phosphate catabolic process_ lactose catabolic process via tagatose-6-phosphate	+1.6	1
UP16	SYD	Aspartate–trna ligase	4.96	66,728	72	A7 × 344	*aspS*	ATP binding_spartate-trna ligase activity_nucleic acid binding	Aspartyl-trna aminoacylation Protein biosynthesis	+0.9	–
UP17	GCH4	GTP cyclohydrolase fole2	5.16	33,631	45	A7WZ02	*folE2*	Gtp cyclohydrolase I activity	7,8-dihydroneopterin 3′-triphosphate biosynthetic process	+1.1	–
UP18	LACB	Galactose-6-phosphate isomerase subunit lacb	5.51	19,141	157	A7 × 578	*lacB*	Galactose-6-phosphate isomerase activity	Galactose catabolic process_lactose catabolic process	+2.8	3
UP19	TKT	Transketolase	4.97	72,206	67	Q5HG77	*tkt*	Metal ion binding_ tranketolase activity	DNA ricombination_ pentose phosphate shunt_reductive pentose-phosphate cycle	+1.4	1

[†]Values are Log_{10} (p), where p is the probability that the observed match is a random event; based on Swiss-Prot and NCBI databases using the MASCOT searching program.
[‡]Based on Swiss-Prot and NCBI databases.
[§]Negative value: Protein downregulation; Positive value: Protein upregulation.
[¶]MS/MS is the number of matched peptides from ion parent fragments.
pI Exp: Isoelectric point as determined from the 2-D gel experiment.

Table 2. Proteins differentially expressed in *Staphylococcus aureus* Sa3 strain after exposure to usnic acid (cont.).

Label	Abbreviated name	Description name	pI theo	Mw theo	Score[†]	Swiss Prot/NCBI AC[‡]	Gene name	Molecular function	Biological process	Fold-change variation[§]	MS/MS[¶]
UP20	TKT	Transketolase	4.97	72,206	179	Q5HG77	*tkt*	Metal ion binding_ tranketolase activity	DNA ricombination_ pentose phosphate shunt_reductive pentose-phosphate cycle	+1.6	1
UP66		NADH:flavin oxidoreductase	5.19	41,971	72	gi|386830499	*SAKOR_00316*	FMN binding_ oxidoreductase activity	Oxidation–reduction process	+1.3	–
UP68	O87364	ParM protein	5.25	38,206	69	gi|487735407	*parM*	Actin polimerization	DNA segregation, Plasmide retention	+0.85	–
DW1	SYFA	Phenylalanyl-trna synthase subunit alpha	5.56	40,363	93	C5N4M2	*pheS*	ATP binding_magnesium ion binding_phenylalanine-trna ligase activity_trna binding	Phenylalanyl-trna amminoacylation	-1.1	–
DW5	FABG	3-oxoacyl-(acyl-carrier-protein) reductase, partial	5.18	24,925	112	Q6G9Y2	*fabG*	3-oxoacyl-(acyl-carrier-protein) reductase (NADPH) activity_NAD binding_ NADP binding	Fatty-acid elongation	-1.3	2
DW6	NAGB	Glucosamine-6-phosphate isomerase	5.33	22,170	243	A7WZ06	*nagB*	Glucosamine-6.phosphate deaminase activity_ hydrolase activity	N-acetylglucosamine metabolic process_N-acetylneuraminate catabolic process_ carbohydrate metabolic process	-1.8	–
DW7	Y1692	Uncharacterized protein SA1692	4.59	18,677	29	P0A0K1	*SA1692*	Hydrolase activity, acting on glycosyl bonds	Response to stress, cells survive	-1.2	2
DW8	MQO2	Malate:quinone oxidoreductase	6.23	56,491	225	Q5HCU5	*mqo2*	Malate dehydrogenase-(menaquinone)activity_ nakate dehydrogenase-(quinone)activity	Tricarboxylic acid cycle	-1	–
DW9	MQO2	Probable malate:quinone oxidoreductase 2	6.12	56,135	83	Q5HCU5	*mqo2*	Malate dehydrogenase (menaquinone) activity_ malate dehydrogenase (quinone) activity	Tricarboxylic acid cycle	-1	3
DW10	SYT	Threonine–trna ligase	5.26	74,455	33	A7 × 3A6	*thrS*	ATP binding_metal ion binding_thereonine-trna ligase activity	Threonyl-trna aminoacylation	-1.3	1

[†]Values are Log_{10} (p), where p is the probability that the observed match is a random event; based on Swiss-Prot and NCBI databases using the MASCOT searching program.
[‡]Based on Swiss-Prot and NCBI databases.
[§]Negative value: Protein downregulation; Positive value: Protein upregulation.
[¶]MS/MS is the number of matched peptides from ion parent fragments.
pI Exp: Isoelectric point as determined from the 2-D gel experiment.

Table 2. Proteins differentially expressed in *Staphylococcus aureus* Sa3 strain after exposure to usnic acid (cont.).

Label	Abbreviated name	Description name	pI theo	Mw theo	Score[†]	Swiss Prot/NCBI AC[‡]	Gene name	Molecular function	Biological process	Fold-change variation[§]	MS/MS[¶]
DW11	GLMS	Glutamine–fructose-6-phosphate aminotransferase (isomerizing)	4.93	65,923	38	Q5HE49	*glmS*	Carbohydrate binding_ glutamine-fructose-6-phosphate transaminase (isomerizing) activity	Carbohydrate biosynthetic process_ glutamine metabolic process	-1.4	–
DW12	GLYA	Serine hydroxy-methyltransferase	5.75	45,315	90	A7 × 4V7	*glyA*	Glycine hydroxymethyl-transferase activity_ pyridoxal phosphate binding	Glycine biosynthetic process from serine_ tetrahydrofolate interconversion	-1.2	1
DW13	PCKA	Phosphoenol-pyruvate carboxy-kinase (ATP)	5.74	59,511	82	A7 × 3N3	*pckA*	ATP binding_metal ion binding_ phosphoenolpyruvate carboxykinase (ATP) activity	Gluconogenesis	-8.5	–
DW14	ROCA	1-pyrroline-5-carboxylate dehydrogenase	4.98	57,003	133	A7 × 6R7	*rocA*	1-pyrroline-5-carboxylate dehydrogenase activity_ oxidoreductase activity, acting on the aldehyde or oxo group of donors, NAD or NADP as acceptor	Glutamate biosynthetic process_proline biosynthetic process_ proline catabolic process to glutamate	-3.4	1
DW129	FABG	3-oxoacyl-(acyl-carrier-protein) reductase fabg	5.58	26,186	74	Q6G9Y2	*fabG*	3-oxoacyl-(acyl-carrier-protein) reductase (NADPH) activity_NAD binding_ NADP binding	Fatty-acid elengation	-1.3	2
DW131	Y2F × 27 (M1539)	Protease I, partial	4.46	18,189	141	gi|578686624	*Q586_02356*	Peptidase activity_ hydrolase_protease	Proteolysis	-1.9	–

[†]Values are Log_{10} (p), where p is the probability that the observed match is a random event; based on Swiss-Prot and NCBI databases using the MASCOT searching program.
[‡]Based on Swiss-Prot and NCBI databases.
[§]Negative value: Protein downregulation; Positive value: Protein upregulation.
[¶]MS/MS is the number of matched peptides from ion parent fragments.
pI Exp: Isoelectric point as determined from the 2-D gel experiment.

Table 3. Proteins exclusively induced in *Staphylococcus aureus* Sa3 strain after exposure to usnic acid.

Label	Abbreviated name	Description name	pI Exp	Mw	Score†	Swiss Prot/NCBI AC‡	Molecular function	Cellular component	Biological process	LIFT (MS_2) Ion parent masses (*m/z*)	Score	Sequence
D1	CE/NDhdy	Acyl esterase	5.23	60,325	103	H3ZVY0/ gi|446527858	Hydrolase activity_ transferase activity, transferring acyl groups other than amino-acyl groups	Membrane	Metabolic process	1595.6712 1665.7296 930.5031	145	K.AMIPWEGLNDMYR.E R.EVAFHGGIPDTGFYR.F K.WLYVHGR.K
D3	CE/NDhdy	Acyl esterase	5.46	64,387	71	gi|387603875	Hydrolase activity_ transferase activity, transferring acyl groups other than amino-acyl groups	Membrane	Metabolic process	1665.7886 930.4999	66	R.EVAFHGGIPDTGFYR.F K.WLYVHGR.K
D4	CE/NDhdy	Acyl esterase	5.23	60,325	144	H3ZVY0/ gi|446527858	Hydrolase activity_ transferase activity, transferring acyl groups other than amino-acyl groups	Membrane	Metabolic process	1595.7277 1665.7942 930.4992	123	K.AMIPWEGLNDMYR.E R.EVAFHGGIPDTGFYR.F K.WLYVHGR.K
D7	UP355	UPF0355 protein	4.86	15,113	41	–	Unknown	–	Unknown	2557.2098 1496.7598	107	K.LHLNDLHDSEISLIST-SGTFSDR.M K.LLTGEDGEHAVLSR.Y
DB	Z3FLB5_ STAAU	HAD family hydrolase, partial	4.44	28,237	30	gi|446108456	Hydrolase activity	–	Metabolic process	1844.8402 1459.6099 1537.7506	190	K.SIGKQDFDEIVDYCR.D K.QDFDEIVDYCR.D K.VMGVDYVANITEAR.I

†Values are Log_{10} (p), where p is probability that the observed match is a random event; based on Swiss-Prot database using the MASCOT searching program.
‡Based on Swiss-Prot and NCBI databases.
AC: Accession number; HAD: Haloacid dehalogenase; pI Exp: isoelectric point as determined from the 2-D gel experiments;PMF: Peptide mass finger.

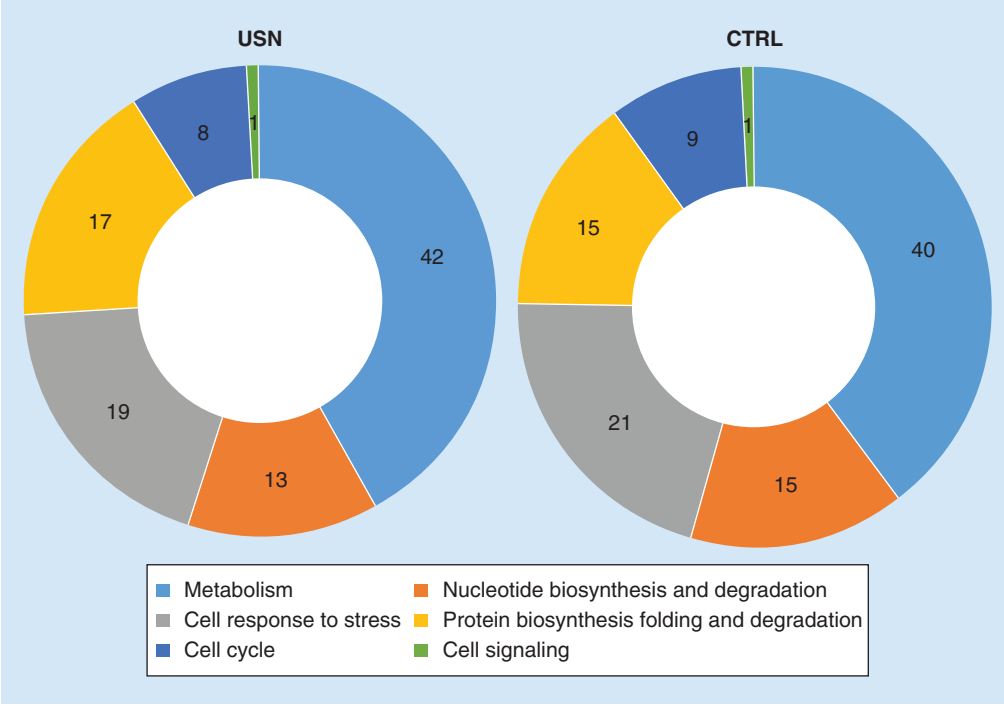

Figure 4. Functional categories of proteins differentially produced by *Staphylococcus aureus* Sa3 strain in response to usnic acid at 1/64 × minimum inhibitory concentration. Gene ontology functional analysis [38] defined six main functional groups, both in usnic acid and control samples: metabolism, nucleotide biosynthesis and degradation, cell response to stress, protein biosynthesis folding and degradation, cell cycle and cell signaling. No statistically significant differences were found in the percentage of each functional group, in USN and CTRL samples. CTRL: Control; USN: Usnic acid.

Particularly, SEM analysis showed that USN exposure at 1/8 × MIC and 1 × MIC concentrations dramatically affects cell survival, as shown by the strong reduction of cells compared with CTRL **(Figure 7A)**. The few aggregates of apparently living cells appear extensively damaged and surrounded by cell debris, likely resulting from cell degeneration **(Figure 7A)**. Contrarily, exposure at 1/64 × MIC had a moderate effect on cell viability **(Figure 7B)**, even though TEM analysis showed a higher number of cells with broken walls, protoplast and cell debris compared with CTRL **(Figure 8A)**.

Morphological investigations highlighted cell shape alterations (i.e., irregular, swollen, oval), extensively damaged wall surface and membrane alterations (i.e., invaginations and discontinuities), all of which were not observed in the untreated control cells. In particular, SEM analysis revealed that USN exposure at 1/64 × MIC caused rough, shrunken surface with irregular folds even in dividing cells **(Figure 7B)**. In addition, TEM evaluation outlined that exposure at 1/64 × MIC produced an increased thickness of the cell wall and marked disorganization, characterized by fibrillary rather than a compact structure as observed in CTRL, as well as induced extensive cell wall breaks presumably causing cell lysis and death **(Figure 8B)**.

• PI uptake assay

To test whether USN caused membrane instability, we added PI to the treated cultures after 24-h exposure. PI, when associated with DNA, fluoresces intensely and its use in this context indicates whether or not *S. aureus* Sa3 membranes are more permeable to PI after treatment. Our data showed that there was a dose-dependent trend, observing a steady increase in fluorescence level with increasing USN concentrations **(Figure 9)**.

Discussion

• Proteomic analysis

The mechanisms underlying the anti-staphylococcal effects of USN are still largely

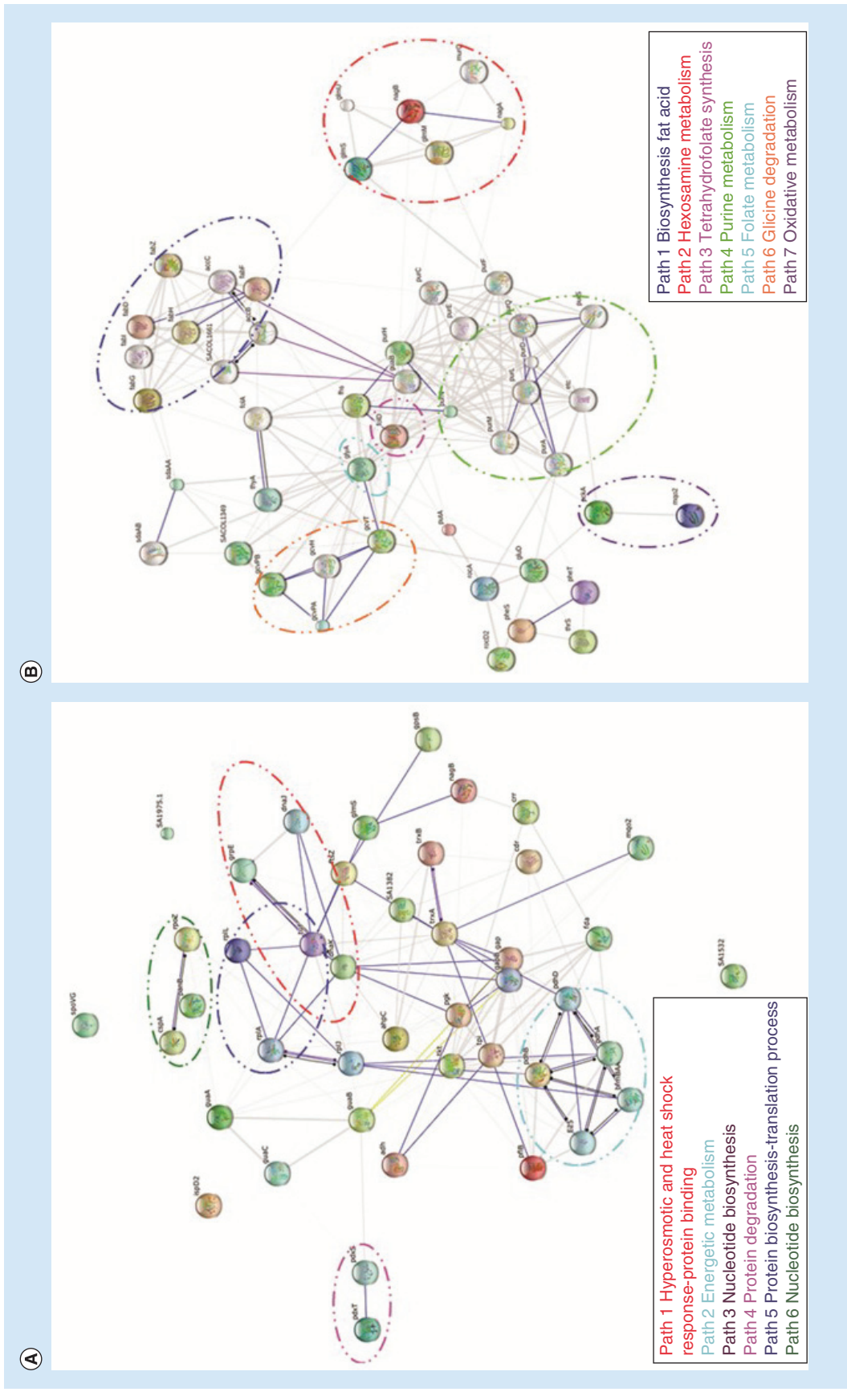

Figure 5. Protein-interaction networks. Protein-interaction network of **(A)** control-related and **(B)** usnic acid-related newly and differentially expressed proteins, extracted using the STRING search tool.

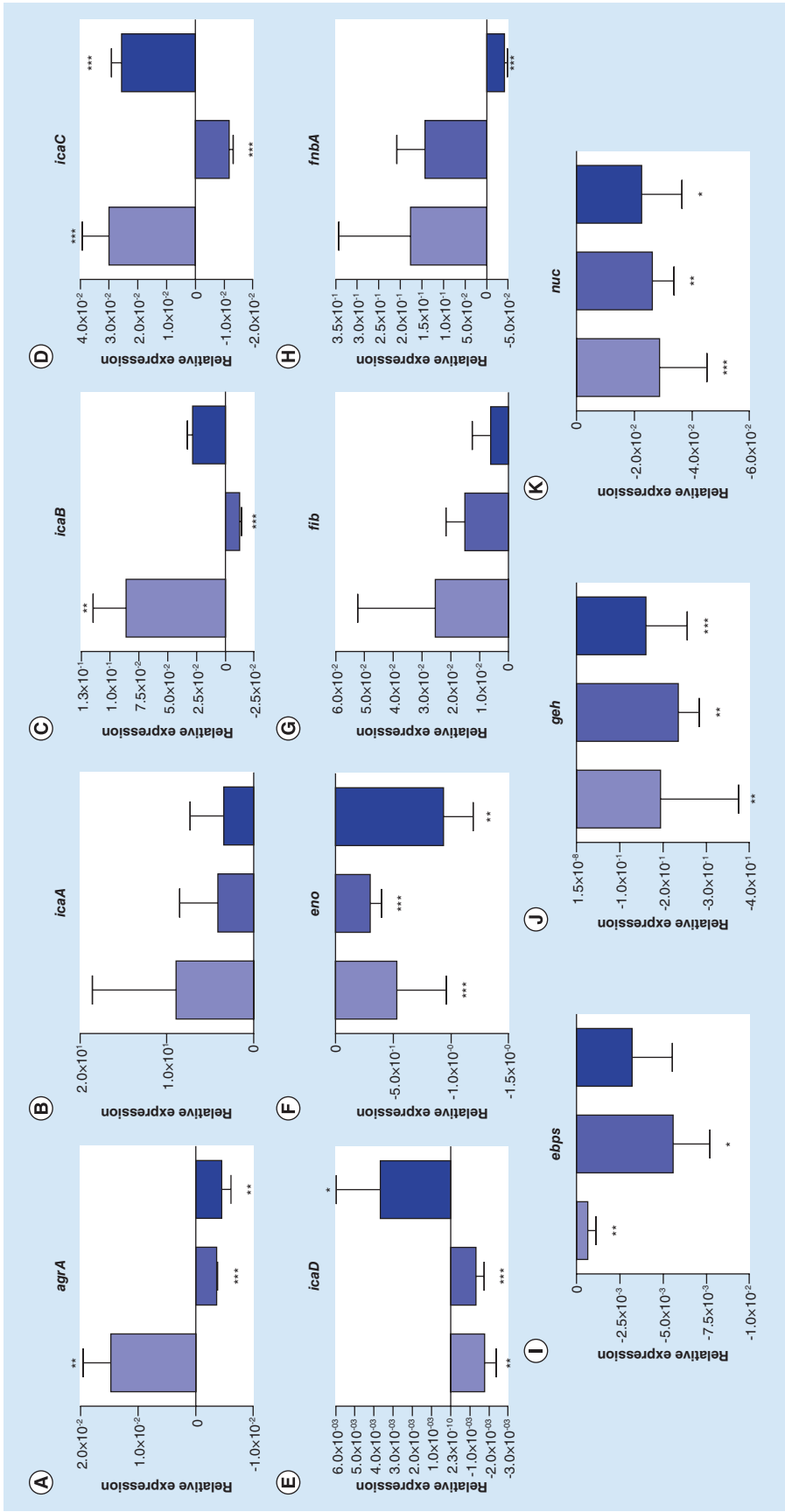

Figure 6. Effect of usnic acid at sub-MICs on the expression levels of 11 virulence genes by *Staphylococcus aureus* Sa3. Cells were exposed (24 h, 37°C) at several subinhibitory usnic acid concentrations (bars, from left to right: 1/256×, 1/128× and 1/64 × minimum inhibitory concentration). Control samples were not exposed to usnic acid but vehicle only. Results are shown as relative expression (n = 6; mean + standard deviation).

* $p < 0.05$ versus control; paired *t*-test.

** $p < 0.01$ versus control; paired *t*-test.

*** $p < 0.001$ versus control; paired *t*-test.

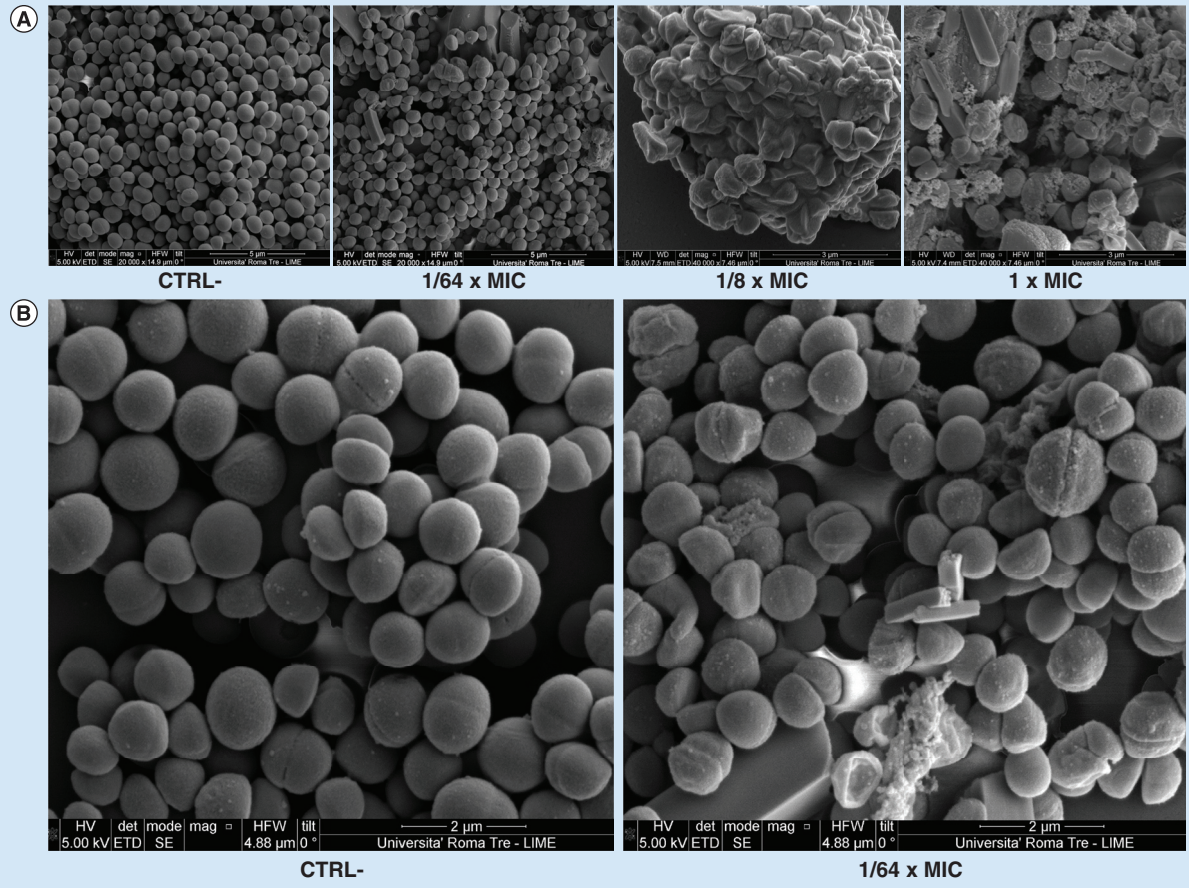

Figure 7. Scanning electron microscopy analysis of *S. aureus* Sa3 exposed to usnic acid at sub-minimum inhibitory concentrations. **(A)** Images show the extensive cell death following exposure to usnic acid at 1/8 × MIC and 1 × MIC. **(B)** Close-ups show the normal, smooth surface of the unexposed cells (CTRL, left), compared with the shrunken surface with irregular folds of the cells exposed to usnic acid at 1/64 × MIC (right).
CTRL: Control (unexposed) sample; MIC: Minimum inhibitory concentration.

unknown and conflicting. Recently, Maciąg-Dorszyńska *et al.* showed that the antibacterial activity of USN is mainly due to inhibition of DNA and RNA synthesis [39]. Different findings were obtained by Gupta *et al.* who observed the disruption of the cell membrane in MRSA strains exposed to USN [40]. No studies have been published with regard to MRSA from CF patients.

The effect of USN at sub-MIC on protein expression by an MRSA strain from CF patient was investigated for the first time in the present study, by identifying newly or differentially expressed proteins through proteomic analysis.

The exposure to USN remarkably decreased the expression of some general metabolic pathway-related proteins based on their functions, as also assessed by Gene Ontology functional analysis. Particularly, we observed a decreased expression of two proteins involved in oxidative metabolism (MQO2 and PCKA), two proteins involved in hexosamine metabolism (glucosamine-6-phosphate isomerase NAGB and glutamine-fructose-6-phosphate aminotransferase GLMS), 3-oxoacyl-reductase acyl-carrier protein FABG (fatty acid biosynthesis), and glycine hydroxymethyltransferase GLYA (folate metabolism).

In addition, there was decreased expression of 1-pyrroline-5-carboxylate dehydrogenase, involved in protein degradation, and the amino-acyl-tRNA synthetase PheRS, an essential enzyme which catalyzes the transfer of phenylalanine to the Phe-specific transfer RNA ($tRNA^{Phe}$), a key step in protein biosynthesis and therefore essential for cell viability. Although structural

and phylogenetic analyses revealed three different forms of PheRS (bacterial heterotetrameric, eukaryotic/archaeal heterotetramic and mitochondrial monomeric), the binding modes and the recognition modes of cognate $tRNA^{Phe}$ are different in prokaryotes and eukaryotes [41]. These findings show that the enzyme is of considerable interest for the development of new antibacterial agents [42]. In particular, the resulting downexpression induced by USN could be detrimental to the cell and thus provide the basis for proposing this secondary metabolite from lichens as a novel antibacterial agent.

It is worthy of note that the affected metabolism of the amino acids (phenylalanine, glycine, glutamate, proline, serine and N-acetylglucosamine) – we observed in USN-treated MRSA cells – may be associated with the decrease in protein and peptidoglycan synthesis since these amino acids are crucial in both biological processes [43,44]. In particular, the reduced glycine content, which is an amino-acid composition of peptidoglycan cross-bridges, might excite the aberrant cell septum formation and retard cell division [45]. Such a possibility is also supported by the data collected with SEM and TEM analyses, as discussed below.

Following treatment with USN at subinhibitory concentrations, *S. aureus* Sa3 strain significantly upregulated the expression of several proteins, such as those involved in oxidative stress and lactose metabolic pathway.

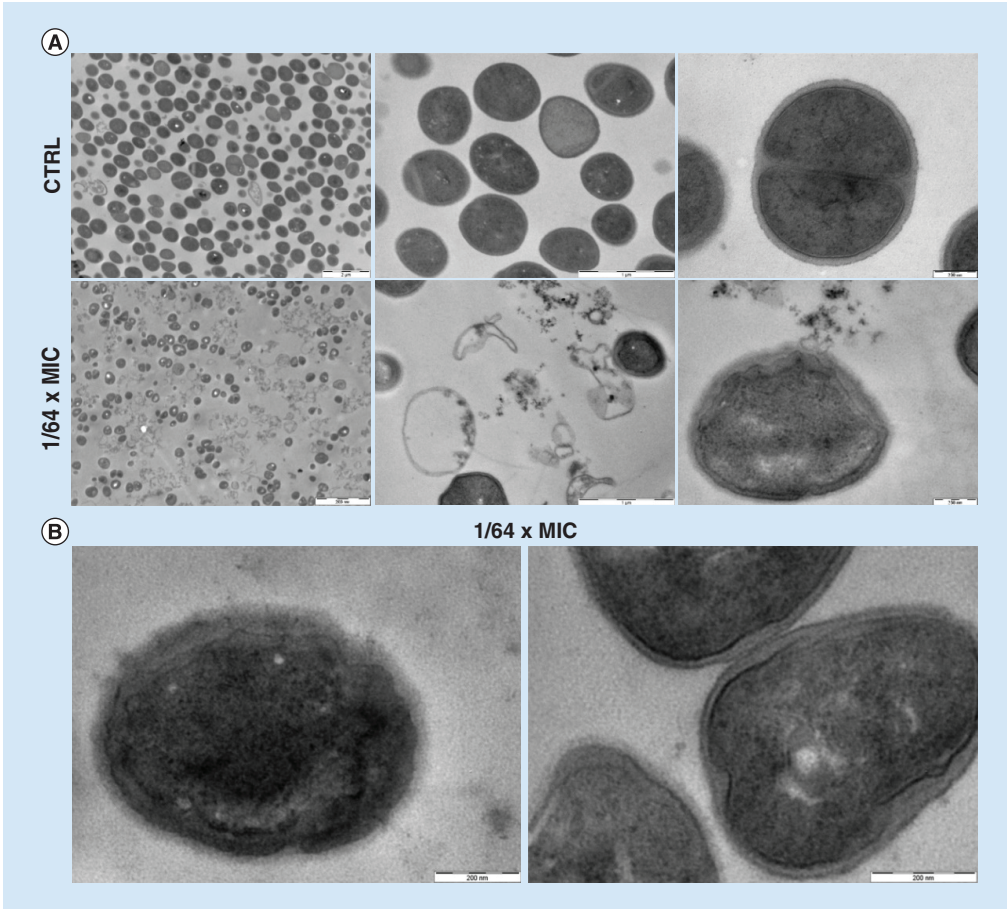

Figure 8. Transmission electron microscopy analysis of *Staphylococcus aureus* Sa3 exposed to usnic acid at 1/64 × MIC. (A) Comparison at different magnifications between unexposed (upper images) and exposed samples to usnic acid at 1/64 × MIC (lower images): note the regularly rounded shape of the CTRL cells compared with the irregular morphology of the exposed cells. **(B)** Close-ups of damaged cells exposed to usnic acid at 1/64 × MIC; note the extensively damaged wall surface and the membrane.
CTRL: Control (unexposed) sample; MIC: Minimum inhibitory concentration.

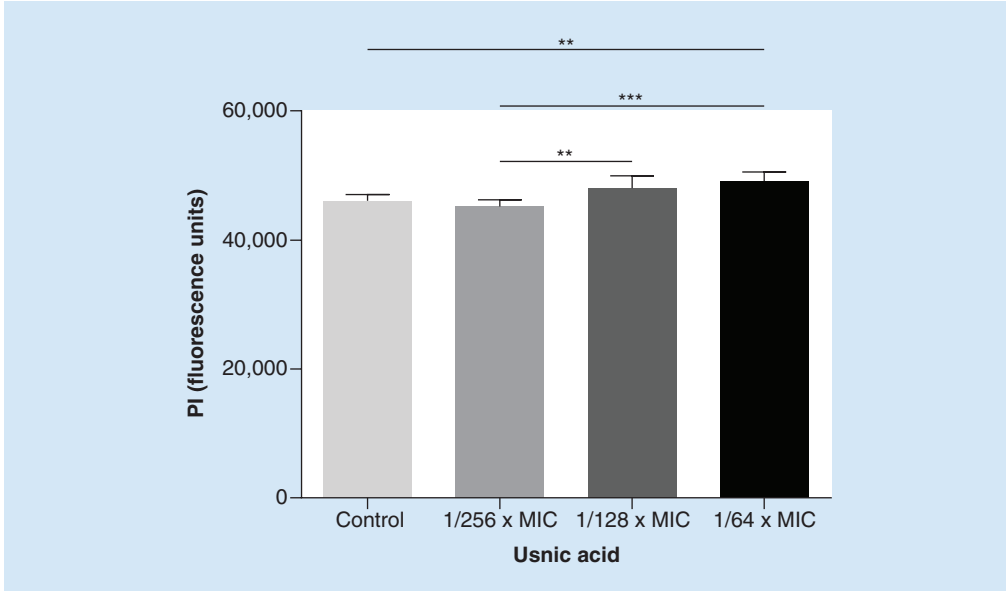

Figure 9. Propidium iodide uptake by *Staphylococcus aureus* Sa3 treated with increasing concentrations of usnic acid. Bacterial cultures were incubated without usnic acid (control) and with three different subinhibitory concentrations of usnic acid. Results are shown as mean + SD (n = 6).
**p < 0.01, ANOVA + Tukey's multiple comparison post-test.
***p < 0.001, ANOVA + Tukey's multiple comparison post-test.
MIC: Minimum inhibitory concentration.

The adaptation of the bacteria to survival under stress conditions is suggested by the increased expression of ScdA and NADH:flavin oxidoreductase proteins. Nitrosative stress, resulting from the enzymatic or non-enzymatic synthesis of NO^-, hypoxia and the perturbation of iron homeostasis cause in fact the induction of genes encoding putative iron-containing proteins, particularly the iron-sulfur SCDA protein, fulfilling crucial redox, catalytic and regulatory functions in virtually all organisms [46–49]. In this picture, the upregulation we observed of GUAA and peptide deformylase could represent a partial compensation for the need to repair damage caused by oxidative stress. GUAA is a putative glutamine amidotransferase of Class I family enzyme with a potential role in purine ribonucleotide biosynthesis [50], while peptide deformylase is needed to remove the formyl moiety from the growing peptide [51]. Both proteins are essential for *S. aureus* growth and virulence [50,51], therefore representing attractive targets for the development of novel antibacterials.

Exposure to USN also upregulated both LACB and LACC proteins. *S. aureus*, *Staphylococcus epidermidis* and *Staphylococcus hominis* are the only organisms known to exclusively use enzymes of the D-tagatose-6-phosphate pathway to metabolize lactose and D-galactose [52]. In *S. aureus*, D-galactose and lactose are imported and metabolized by proteins encoded by the lactose operon, *lacABCDFEG* [53].

Partition or segregation is the essential process whereby the genetic material is actively distributed into daughter cells. In prokaryotes, type II plasmid partition systems utilize ParM NTPases in coordination with a centromere-binding protein called ParR to mediate accurate DNA segregation, a process critical for plasmid retention [54]. Our data indicated that USN, by increasing ParM expression, could therefore facilitate the acquisition of antibiotic resistance elements in *S. aureus* as well as the transfer of virulence factor genes [55,56].

With regard to the proteins specifically induced in the Sa3 strain following treatment with USN, it is worth noting the presence of two isoforms of the Acyl-CoA esterase family, involved in the synthesis of Phase II of long-chain fatty acids, especially in the biogenetic process of the bacterial cell wall [57]. This is highly suggestive of a cell-wall repair mechanism, thus confirming our previous proteomic and ultrastructural observations. FAS-II bacterial fatty-acid biosynthesis pathway is highly conserved across many bacterial systems since its high

affinity for longchain fatty acids enables bacteria to grow and survive in environments with high concentrations of acyl-esters as a C source [58–60].

In addition, Acyl-Coa esterase could also interact with other lipolytic enzymes to digest environmental lipids, therefore enhancing staphylococcal virulence [57]. Taking into account the essentiality of FAS-II pathways for MRSA [61], this system could be considered a possible target for the development of new antibacterial drugs [60,62].

Furthermore, the comparative evaluation of Protein Interactive Networks obtained for CTRL and USN samples interestingly revealed that the exposure to USN causes the lack of some proteins, such as RpoZ and CspA. It has recently been shown that RNA polymerase enzyme (RpoZ) is crucial for biofilm synthesis in *Mycobacterium smegmatis* because of a deficiency in generating the extracellular matrix [63]. USN could, therefore, affect the adhesive ability of planktonic cells by reducing extracellular matrix synthesis and, consequently, counteract biofilm formation.

CspA is a small cold shock protein involved in cell response to stress [64]; in particular, it belongs to a family acting as regulator of protein biosynthesis or specifically in transcription and translation mechanisms involved in cell protection at low temperatures.

• Electron microscopy analyses

The morphological evaluation performed by SEM and TEM analyses clearly revealed that USN dramatically affects *S. aureus* viability in a dose-dependent manner. Growth in the presence of USN generated profound abnormalities in both *S. aureus* morphology and ultrastructure. In agreement with the proteomic findings, USN mainly caused cell-wall damage in *S. aureus* with thickenings, folding and breaks. The PI uptake assay further confirmed this mechanism of action showing that there was a dose-dependent membrane permeability to PI following exposure to USN.

A similar increase in cell-wall thickness was previously observed in staphylococci following exposure to some antibiotics, such as chloramphenicol and penicillin [65]. Overall, these results suggest that cells with thickened wall may represent a defensive response to USN and its mechanism of action.

• Virulence (biofilm) gene expression

As for other Gram-positive bacteria, the pathogenicity of *S. aureus* is mainly dependent upon the secretion of numerous extracellular virulence factors. Consequently, the efficacy of antibiotic therapy for the treatment of *S. aureus* infections relies not only on their respective bactericidal or bacteriostatic activities but also on their ability to affect the release of virulence factors. An alternative therapeutic strategy could therefore be based on the reduction of bacterial pathogenicity rather than on placing immediate life-or-death pressure on the target bacterium [66].

The virulence factors employed by *S. aureus* to cause diseases consist of cell wall surface-exposed and secreted proteins, such as lipase and thermonuclease [67–69]. Lipase functions in virulence by degrading lipids in order to help the bacterium acquire nutrients, and its expression is higher in strains causing deep infections (i.e., septicemia, osteomyelitis) rather than in those associated with superficial ones (i.e., impetigo, or from nasal mucosa) [70]. Thermonuclease is involved in facilitating the escape of *S. aureus* from neutrophil extracellular traps, and contributes to disease pathogenesis in a murine respiratory tract infection model [69]. The role of these enzymes in *S. aureus* CF pathogenesis has yet to be studied. Recently, it has been observed that lipase activity is highly maintained in the *B. cepacia* complex and that it could have a potential role in lung epithelial cell invasion [71].

Our data clearly showed that exposure to subinhibitory USN concentrations causes significant reduction of *nuc* and *geh* expression, therefore suggesting that the structure of this secondary metabolite from lichens could be used as a fundamental structure for the development of antimicrobial agents aimed at the reduction of bacterial virulence.

The adhesion of bacteria to host cells or indwelling medical devices is an important prerequisite for both infection and the initiation of biofilm formation. The adherence stage of *S. aureus* to both the native tissues and abiotic surfaces is mediated by a protein family of staphylococcal microbial surface components recognizing adhesive matrix molecules, such as fibronectin binding proteins (FnbA and FnbB), laminin binding protein (Eno), elastin binding protein (EbpS) and fibrinogen binding protein (Fib) [72–74].

We recently observed that *in vitro* USN is able to prevent the formation of biofilms and to disrupt established biofilms by *S. aureus* strains isolated from CF patients [24]. To gain new insights in the mechanisms underlying this antibiofilm

activity, real-time RT-PCR was carried out to evaluate the effect of subinhibitory USN concentrations on the expression of several genes encoding products involved in *S. aureus* biofilm formation. Our results indicated that exposure to USN significantly reduces the transcription of the gene encoding adhesins for the host matrix binding proteins elastin, laminin and fibronectin by MRSA Sa3 strain – a strong indication that USN impairs the efficacy of ligand binding needed for the bacterial cells to adhere to host and further reduces infection initiation and biofilm formation.

The well-known relationship between the chronicization of infection and the presence of biofilm in CF patients [75], reinforces the clinical relevance of antibiofilm effects of USN.

This effect does not seem to involve the fibrinogen receptor, although the lack of statistical significance could be mainly due to the high variability of data obtained. The mechanism underlying antibiofilm activity of USN could also involve a decreased lipase and thermonuclease expression. It has been in fact observed that lipase encoding genes were induced and found to be among the upregulated genes involved in biofilm formation in *S. aureus* [76]. Lipase inhibitors such as farnesol and antilipase serum have been demonstrated to reduce biofilm formation in *S. aureus* [77,78]. Recently, studies have shown that *S. aureus* Nuc secretion controls biofilm, remodeling the eDNA matrix acting as a biofilm inhibitor [79].

The activation of the quorum-sensing system *agr* has a negative impact on biofilm formation in *S. aureus*. Agr activation results in fact in the expression of extracellular proteases and membrane-active molecules that both contribute to the dispersal of biofilms [80]. Our results showed that the effect of USN on *agrA* expression is concentration-dependent, resulting decreased in the presence of concentrations at 1/64× and 1/128 × MIC, while increased at 1/256 × MIC. Further studies are needed for a better comprehension of these findings.

Conclusion & future perspective

The present work explored the anti-staphylococcal mode of action of USN by using, for the first time in literature, an integrated approach consisting of proteomic, genomic and ultrastructural analyses.

Overall, our results showed that USN: exerts its anti-staphylococcal effect mainly through cell-wall damage and inhibition of bacterial growth, mainly due to reduced amino-acid biosynthesis, and protein synthesis; affects *S. aureus* adhesion (the early stages of biofilm formation) by reducing both the synthesis of adhesins for the host matrix binding proteins, and the bacterial extracellular matrix; reduces the pathogenic potential of *S. aureus* also by affecting the expression of relevant virulence factors, such as lipase and thermonuclease.

Taken together, our findings provide a theoretical basis for the potential application of USN as a therapeutic agent against MRSA infections that increase morbidity, mortality healthcare costs, whose control continues to be an unresolved issue in many hospitals worldwide. The use of USN in fact could offer new perspectives into both prevention and treatment of biofilm-related and difficult-to-treat staphylococcal chronic lung infections in CF patients. USN could be used as a 'probe' for the identification of new targets for antimicrobials. In this regard, the present study has provided new insights on the mechanism of action of USN, therefore, paving the way for the identification of new molecular targets. The identification and characterization of novel objectives and new lead compounds for chemotherapy could lead to the development of more effective antibiotics which could delay resistance. Although the use of USN in therapeutic application is rather limited due to toxicity issues, its encapsulation could maintain and improve its biological activity while considerably reducing the toxicity of this drug [20]. Further investigations are, therefore, warranted to understand the real therapeutic potential of USN by means of *in vivo* models and well-designed, evidence-based, randomized clinical studies.

Acknowledgements

The authors thank Prof S Moreno (Department of Science – LIME, University Roma Tre, Rome, Italy) for technical assistance and helpful suggestions on the electron microscopy analysis, Prof PG Righetti (Department of Chemistry Materials and Chemical Engineering 'Giulio Natta', Politecnico di Milano, Milan, Italy) for his valuable revision of the manuscript, and Rachel Price and Sandra Cicchitti (English Reader, Linguistic Center, 'G d'Annunzio' University of Chieti) who assisted in the proof-reading of the manuscript with no charge.

Author contributions

G Di Bonaventura, S Angelucci and C Di Ilio designed the research, analyzed and wrote the paper; A Pompilio,

A Riviello, V Crocetta, F Di Giuseppe, S Pomponio, M Sulpizio, L Barone and A Di Giulio performed the experiments.

No writing assistance was utilized in the production of this manuscript.

Financial & competing interests disclosure

This work was supported by a grant from the 'G. d'Annunzio' University of Chieti-Pescara ("quota ex-60%", anno 2014). The authors have no other relevant affiliations or financial involvement with any organization or entity with financial interest in or financial conflict with the subject matter or materials discussed in the manuscript apart from those disclosed.

Ethical conduct of research

The work described in this study focused on a strain collected during routine diagnostic activity. The authors state that they have obtained appropriate institutional review board approval or have followed the principles outlined in the Declaration of Helsinki for all human or animal experimental investigations. In addition, for investigations involving human subjects, informed consent has been obtained from the participants involved.

EXECUTIVE SUMMARY

- Methicillin-resistant *Staphylococcus aureus* (MRSA) is an important emerging pathogen in cystic fibrosis (CF) patients, where it causes persistent lung infections leading to a decline in lung function, despite appropriate anti-staphylococcal therapy.
- In addition to methicillin resistance, another adaptive strategy adopted by *S. aureus* to survive in CF lung is the formation of biofilm, sessile communities inherently resistant to antimicrobial agents and host immunity.
- The relevant morbidity and mortality associated with *S. aureus* infection and the increased antibiotic resistance demand new antimicrobial strategies to be urgently developed.
- Usnic acid (USN), a compound that typically arises from the secondary metabolism of the fungal component of lichens, affects growth and biofilm formation by MRSA CF strains.
- Understanding the mode of action of USN could pave the way for the identification of new molecular targets for innovative antimicrobials.
- Proteomic analysis showed that USN exerts its antibacterial function mainly through cell-wall damage and inhibition of bacterial growth, mainly due to reduced amino acid biosynthesis and protein synthesis.
- SEM and TEM analyses confirmed that USN dramatically affects *S. aureus* viability due to cell-wall damage with thickenings, folding and breaks.
- RT-PCR results revealed that USN can reduce the pathogenic potential of *S. aureus*, both decreasing biofilm formation ability (secondary to an impaired early adhesion to host mucosa) and affecting the expression of relevant virulence factors such as lipase and thermonuclease.
- USN could be considered for the development of an alternative therapeutic strategy against MRSA infections, based on both antibacterial activity and reduction of bacterial pathogenicity. Furthermore, *in vivo* animal and clinical studies are warranted for this aim.

References

Papers of special note have been highlighted as:
• of interest; •• of considerable interest.

1 Cystic Fibrosis Foundation Patient Registry. 2008 Annual Data Report. Cystic Fibrosis Foundation, MD, USA (2009).

2 Goodrich JS, Sutton-Shields TN, Kerr A, Wedd JP, Miller MB, Gilligan PH. Prevalence of community-associated methicillin-resistant *Staphylococcus aureus* in patients with cystic fibrosis. *J. Clin. Microbiol.* 47(4), 1231–1233 (2009).

3 Dasenbrook EC, Merlo CA, Diener-West M, Lechtzin N, Boyle MP. Persistent methicillin-resistant *Staphylococcus aureus* and rate of *FEV1* decline in cystic fibrosis. *Am. J. Respir. Crit. Care Med.* 178(8), 814–821 (2008).

4 Branger C, Gardye C, Lambert-Zechovsky N. Persistence of *Staphylococcus aureus* strains among cystic fibrosis patients over extended periods of time. *J. Med. Microbiol.* 45, 294–301 (1996).

5 Kahl BC, Duebbers A, Lubritz G *et al.* Population dynamics of persistent *Staphylococcus aureus* isolated from the airways of cystic fibrosis patients during a 6-year prospective study. *J. Clin. Microbiol.* 41, 4424–4427 (2003).

6 Sawicki GS, Rasouliyan L, Ren CL. The impact of MRSA on lung function in patients with cystic fibrosis. *Am. J. Respir. Crit. Care Med.* 179(8), 734–735 (2009).

7 Goerke C, Wolz C. Adaptation of *Staphylococcus aureus* to the cystic fibrosis lung. *Int. J. Med. Microbiol.* 300(8), 520–525 (2010).

8 Molina A, Del Campo R, Máiz L, Morosini MI, Lamas A, Baquero F. High prevalence in cystic fibrosis patients of multiresistant hospital-acquired methicillin-resistant *Staphylococcus aureus* ST228-SCCmecI capable of biofilm formation. *J. Antimicrob. Chemother.* 62, 961–967 (2008).

9 Besier S, Smaczny C, von Mallinckrodt C *et al.* Prevalence and clinical significance of

Staphylococcus aureus small-colony variants in cystic fibrosis lung disease. *J. Clin. Microbiol.* 45(1), 168–172 (2007).

10 Hunek S. The significance of lichens and their metabolites. *Naturwissenschaften* 86, 559 (1999).

11 Cocchietto M. A review on usnic acid, an interesting natural compound. *Naturwissenschaften* 89, 137 (2002).

12 Ingòlfsdòttir K. Usnic acid. *Phytochemistry* 61, 729 (2002).

13 Lautwerwein M, Oethinger M, Belsner K, Peters T, Marre R. *In vitro* activities of the lichen secondary metabolites vulpinic acid, (+)-usnic acid, and (-)-usnic acid against aerobic and anaerobic microorganisms. *Antimicrob. Agents Chemother.* 39, 2541–2543 (1995).

14 Shibata S, Ukita T, Tamura T, Miura Y. Relation between chemical constitutions and antibacterial effects of usnic acid and derivates. *Jpn. Med. J.* 1, 152–155 (1948).

15 Nithyanand P, Beema Shafreen RM, Muthamil S, Karutha Pandian S. Usnic acid inhibits biofilm formation and virulent morphological traits of *Candida albicans*. *Microbiol. Res.* 179, 20–28 (2015).

16 Nithyanand P, Beema Shafreen RM, Muthamil S, Karutha Pandian S. Usnic acid, a lichen secondary metabolite inhibits Group A *Streptococcus* biofilms. *Antonie Van Leeuwenhoek* 107(1), 263–272 (2015).

17 Araújo AA, de Melo MG, Rabelo TK *et al.* Review of the biological properties and toxicity of usnic acid. *Nat. Prod. Res.* 29(23), 2167–2180 (2015).

18 Brisdelli F, Perilli M, Sellitri D *et al.* Cytotoxic activity and antioxidant capacity of purified lichen metabolites: an *in vitro* study. *Phytother. Res.* 27(3), 431–437 (2013).

19 Taresco V, Francolini I, Padella F *et al.* Design and characterization of antimicrobial usnic acid loaded-core/shell magnetic nanoparticles. *Mater. Sci. Eng. C. Mater. Biol. Appl.* 52, 72–81 (2015).

20 da Silva Santos NP, Nascimento SC, Wanderley MS *et al.* Nanoencapsulation of usnic acid: an attempt to improve antitumour activity and reduce hepatotoxicity. *Eur. J. Pharm. Biopharm.* 64(2), 154–160 (2006).

21 Grumezescu AM, Cotar AI, Andronescu E *et al. In vitro* activity of the new water-dispersible Fe_3O_4-usnic acid nanostructure against planktonic and sessile bacterial cells. *J. Nanoparticle Res.* 15, 1766–1776 (2013).

22 Grumezescu V, Holban AM, Grumezescu AM *et al.* Usnic acid-loaded biocompatible magnetic PLGA–PVA microsphere thin films fabricated by MAPLE with increased resistance to staphylococcal colonization. *Biofabrication*, 6, 1–12 (2014).

23 Francolini I, Norris P, Piozzi A, Donelli G, Stoodley P. Usnic acid, a natural antimicrobial agent able to inhibit bacterial biofilm formation on polymer surfaces. *Antimicrob. Agents Chemother.* 48(11), 4360–4365 (2004).

24 Pompilio A, Pomponio S, Di Vincenzo V *et al.* Antimicrobial and antibiofilm activity of secondary metabolites of lichens against methicillin-resistant *Staphylococcus aureus* strains from cystic fibrosis patients. *Future Microbiol.* 8(2), 281–292 (2013).

• **Usnic acid, at concentrations significantly lower than those causing hepatotoxic effects in animals, affects both biofilm formation and preformed mature biofilms by *S. aureus* isolated from cystic fibrosis patients.**

25 Strommenger B, Kettlitz C, Werner G, Witte W. Multiplex PCR assay for simultaneous detection of nine clinically relevant antibiotic resistance genes in *Staphylococcus aureus*. *J. Clin. Microbiol.* 41, 4089–4094 (2003).

26 Clinical and Laboratory Standards Institute. Performance standards for antimicrobial susceptibility testing; twentieth informational supplement, M100-S20. Clinical and Laboratory Standards Institute, PA, USA (2010). http://shop.clsi.org/

27 Antonioli P, Bachi A, Fasoli E, Righetti PG. Efficient removal of DNA from proteomic samples prior to two-dimensional map analysis. *J. Chromatography A* 1216(17), 3606–3612 (2009).

28 Mao S, Luo Y, Bao G, Zhang Y, Li Y, Ma Y. Comparative analysis on the membrane proteome of *Clostridium acetobutylicum* wild type strain and its butanol-tolerant mutant. *Mol. Biosyst.* 7, 1660–1677 (2011).

29 Sulpizio M, Falone S, Amicarelli F *et al.* Molecular basis underlying the biological effects elicited by extremely low-frequency magnetic field (ELF-MF) on neuroblastoma cells. *J. Cell Biochem.* 112(12), 3797–3806 (2011).

30 STRING. http://string-db.org

31 ExPASy. Bioinformatics Resource Portal. www.expasy.org

32 Livak KJ, Schmittgen TD. Analysis of relative gene expression data using real-time quantitative PCR and the 2-ΔCt method. *Methods* 25, 402–408 (2001).

33 Atshan SS, Shamsudin MN, Karunanidhi A *et al.* Quantitative PCR analysis of genes expressed during biofilm development of methicillin resistant *Staphylococcus aureus* (MRSA). *Infect. Genet. Evol.* 18, 106–112 (2013).

34 Qiu J, Feng H, Lu J *et al.* Eugenol reduces the expression of virulence-related exoproteins in *Staphylococcus aureus*. *Appl. Environ. Microbiol.* 76(17), 5846–5851 (2010).

35 Mitchell G, Lafrance M, Boulanger S *et al.* Tomatidine acts in synergy with aminoglycoside antibiotics against multiresistant *Staphylococcus aureus* and prevents virulence gene expression. *J. Antimicrob. Chemother.* 67(3), 559–568 (2012).

36 Pompilio A, Catavitello C, Picciani C *et al.* Subinhibitory concentrations of moxifloxacin decrease adhesion and biofilm formation of *Stenotrophomonas maltophilia* from cystic fibrosis. *J. Med. Microbiol.* 59(Pt 1), 76–81 (2010).

37 Di Bonaventura G, Spedicato I, D'Antonio D, Robuffo I, Piccolomini R. Biofilm formation by *Stenotrophomonas maltophilia*: modulation by quinolones, trimethoprim-sulfamethoxazole, and ceftazidime. *Antimicrob. Agents Chemother.* 48(1), 151–160 (2004).

38 Gene Oncology Consortium. http://geneontology.org

39 Maciąg-Dorszyńska M, Węgrzyn G, Guzow-Krzemińska B. Antibacterial activity of lichen secondary metabolite usnic acid is primarily caused by inhibition of RNA and DNA synthesis. *FEMS Microbiol. Lett.* 353(1), 57–62 (2014).

40 Gupta VK, Verma S, Gupta S *et al.* Membrane-damaging potential of natural L-(-)-usnic acid in *Staphylococcus aureus*. *Eur. J. Clin. Microbiol. Infect. Dis.* 31, 3375–3383 (2012).

41 Mermershtain I, Finarov I, Klipcan L, Kessler N, Rozenberg H, Safro MG. Idiosyncrasy and identity in the prokaryotic Phe-system: crystal structure of *Escherichia coli* phenylalanyl-tRNA synthetase complexed with phenylalanine and AMP. *Protein Sci.* 20(1), 160–167 (2011).

•• **The modes of binding and of the recognition of cognate $tRNA^{Phe}$ are different in prokaryotes and eukaryotes, therefore making phenylalanyl-tRNA synthetase of considerable promise for creation of new antibacterial agents.**

42 Beyer D, Kroll HP, Endermann R *et al.* New class of bacterial phenylalanyl-tRNA synthetase inhibitors with high potency and broad-spectrum activity. *Antimicrob. Agents Chemother.* 48(2), 525–532 (2004).

43 de Jonge BL, Chang YS, Gage D, Tomasz A. Peptidoglycan composition of a highly methicillin-resistant *Staphylococcus aureus* strain. The role of penicillin binding protein 2A. *J. Biol. Chem.* 267, 11248–11254 (1992).

44 Maidhof H, Reinicke B, Blumel P, Berger-Bachi B, Labischinski H. femA, which encodes a factor essential for expression of methicillin resistance, affects glycine content of peptidoglycan in methicillin-resistant and methicillin susceptible *Staphylococcus aureus* strains. *J. Bacteriol.* 173, 3507–3513 (1991).

45 Gustafson JE, Berger-Bachi B, Strassle A, Wilkinson BJ. Autolysis of methicillin-resistant and -susceptible *Staphylococcus aureus*. *Antimicrob. Agents Chemother.* 36, 566–572 (1992).

46 Johnson DC, Dean DR, Smith AD, Johnson MK. Structure, function, and formation of biological iron-sulfur clusters. *Annu. Rev. Biochem.* 74, 247–281 (2005).

47 Kiley PJ, Beinert H. The role of Fe-S proteins in sensing and regulation in bacteria. *Curr. Opin. Microbiol.* 6, 181–185 (2003).

48 Chang W, Small DA, Toghrol F, Bentley WE. Global transcriptome analysis of *Staphylococcus aureus* response to hydrogen peroxide. *J. Bacteriol.* 188, 1648–1659 (2006).

49 Richardson AR, Dunman PM, Fang FC. The nitrosative stress response of *Staphylococcus aureus* is required for resistance to innate immunity. *Mol. Microbiol.* 61, 927–939 (2006).

50 Mulhbacher J, Brouillette E, Allard M, Fortier LC, Malouin F, Lafontaine DA. Novel riboswitch ligand analogs as selective inhibitors of guanine-related metabolic pathways. *PLoS Pathog.* 6(4), e1000865 (2010).

51 Margolis PS, Hackbarth CJ, Young DC *et al.* Peptide deformylase in *Staphylococcus aureus*: resistance to inhibition is mediated by mutations in the formyltransferase gene. *Antimicrob. Agents Chemother.* 44(7), 1825–1831 (2000).

52 Götz F, Schleifer KH. Biochemical properties and the physiological role of the fructose-1,6-bisphosphate activated L-lactate dehydrogenase from *Staphylococcus epidermidis*. *Eur. J. Biochem.* 90(3), 555–561 (1978).

53 Rosey EL, Oskouian B, Stewart GC. Lactose metabolism by *Staphylococcus aureus*: characterization of *lacABCD*, the structural genes of the tagatose 6-phosphate pathway. *J. Bacteriol.* 173(19), 5992–98 (1991).

54 Hayes F, Barillà D. The bacterial segrosome: a dynamic nucleoprotein machine for DNA trafficking and segregation. *Nat. Rev. Microbiol.* 4(2), 133–43 (2006).

55 Omoe K, Hu DL, Takahashi-Omoe H, Nakane A, Sinagawa K. Identification and characterization of a new staphylococcal enter toxin-related putative toxin encoded by two kinds of plasmids. *Infect. Immun.* 71, 6088–6094 (2003).

56 Firth N, Skurray RA. *Gram-positive pathogens*. Fischetti VA, Novick RP, Ferretti JJ, Portnoy DA, Rood JI (Eds), American Society for Microbiology, Washington, DC, USA, 413–426 (2006).

57 Ohkawa I, Shiga S, Kageyama M. An esterase on the outer membrane of *Pseudomonas aeruginosa* for the hydrolysis of long chain acyl esters. *J. Biochem.* 86(3), 643–656 (1979).

58 Parsons JB1, Frank MW, Subramanian C, Saenkham P, Rock CO. Metabolic basis for the differential susceptibility of Gram-positive pathogens to fatty acid synthesis inhibitors. *Proc. Natl Acad. Sci. USA* 108(37), 15378–15383 (2011).

•• **Contrarily to other Gram-positive bacteria, in *S. aureus* exogenous fatty acids are not able to shut off *de novo* biosynthesis, and this accounts for their sensitivity to FASII inhibitors even in the presence a fatty-acid supplement.**

59 Payne DJ, Warren PV, Holmes DJ, Lonsdale JT. Bacterial fatty-acid biosynthesis: a genomics-driven target for antibacterial drug discovery. *Drug Disc. Today* 6(10), 537–544 (2001).

• **An integrated approach consisting of genomics, bioinformatics and genomic technologies has enabled an in-depth analysis of the component enzymes of the bacterial fatty-acid biosynthesis pathway as a source of novel antibacterial targets.**

60 Campbell JW, Cronan JE Jr. Bacterial fatty acid biosynthesis: targets for antibacterial drug discovery. *Annu. Rev. Microbiol.* 55, 305–332 (2001).

61 Balemans W, Lounis N, Gilissen R *et al.* Essentiality of FASII pathway for *Staphylococcus aureus*. *Nature* 463(7279), E3; discussion E4 (2010).

62 Parsons JB, Rock CO. Is bacterial fatty acid synthesis a valid target for antibacterial drug discovery? *Curr. Opin. Microbiol.* 14(5), 544–549 (2011).

63 Mathew R, Mukherjee R, Balachandar R, Chatterji D. Deletion of the *rpoZ* gene, encoding the omega subunit of RNA polymerase, results in pleiotropic surface-related phenotypes in *Mycobacterium smegmatis*. *Microbiology* 152, 1741–1750 (2006).

64 Kaufman-Szymczyk A, Wojtasik A, Parniewski P, Białkowska A, Tkaczuk K, Turkiewicz M. Identification of the *csp* gene and molecular modelling of the CspA-like protein from Antarctic soil-dwelling psychrotrophic bacterium *Psychrobacter* sp. B6. *Acta Biochim. Pol.* 56(1), 63–69 (2009).

65 Giesbrecht P, Kersten T, Maidhof H, Wecke J. Staphylococcal cell wall: morphogenesis and fatal variations in the presence of penicillin. *Microbiol. Mol. Biol. Rev.* 62, 1371–1414 (1998).

66 Cegelski L, Marshall GR, Eldridge GR, Hultgren SJ. The biology and future prospects of antivirulence therapies. *Nat. Rev. Microbiol.* 6, 17–27 (2008).

•• **Exhaustive review of the efforts toward antivirulence-based drug discovery in the framework of marketable drugs, and discussion of the challenges and factors crucial to developing the antivirulence therapeutic approach.**

67 Hu C, Xiong N, Zhang Y, Rayner S, Chen S. Functional characterization of lipase in the pathogenesis of *Staphylococcus aureus*. *Biochem. Biophys. Res. Commun.* 419(4), 617–620 (2012).

68 Sibbald MJ, Ziebandt AK, Engelmann S *et al.* Mapping the pathways to staphylococcal pathogenesis by comparative secretomics. *Microbiol. Mol. Biol. Rev.* 70, 755–788 (2006).

69 Berends ET, Horswill AR, Haste NM, Monestier M, Nizet V, von Köckritz-Blickwede M. Nuclease expression by *Staphylococcus aureus* facilitates escape from neutrophil extracellular traps. *J. Innate Immun.* 2(6), 576–586 (2010).

70 Rollof J, Hedström SA, Nilsson-Ehle P. Lipolytic activity of *Staphylococcus aureus* strains from disseminated and localized infections. *Acta Pathol. Microbiol. Immunol. Scand. B.* 95(2), 109–113 (1987).

71 Mullen T, Markey K, Murphy P, McClean S, Callaghan M. Role of lipase in *Burkholderia cepacia complex* (Bcc) invasion of lung epithelial cells. *Eur. J. Clin. Microbiol. Infect. Dis.* 26(12), 869–877 (2007).

72 Nakakido M, Aikawa C, Nakagawa I, Tsumoto K. The staphylococcal elastin-binding protein regulates zinc-dependent growth/biofilm formation. *J. Biochem.* 156(3), 155–162 (2014).

73 Speziale P, Pietrocola G, Foster TJ, Geoghegan JA. Protein-based biofilm matrices in

staphylococci. *Front. Cell Infect. Microbiol.* 4, 171 (2014).

74 McCourt J, O'Halloran DP, McCarthy H, O'Gara JP, Geoghegan JA. Fibronectin-binding proteins are required for biofilm formation by community-associated methicillin-resistant *Staphylococcus aureus* strain LAC. *FEMS Microbiol. Lett.* 353(2), 157–164 (2014).

75 Cullen L, McClean S. Bacterial adaptation during chronic respiratory infections. *Pathogens* 4(1), 66–89 (2015).

76 Lowe AM, Beattie DT, Deresiewicz RL. Identification of novel staphylococcal virulence genes by *in vivo* expression technology. *Mol. Microbiol.* 27, 967–976 (1998).

77 Jabra-Rizk MA, Meiller TF, James CE *et al.* Effect of farnesol on *Staphylococcus aureus* biofilm formation and antimicrobial susceptibility *Antimicrob. Agents Chemother.* 50, 1463–1469 (2006).

78 Xiong N, Hu C, Zhang Y, Chen SL. Interaction of sortase A and lipase 2 in the inhibition of *Staphylococcus aureus* biofilm formation. *Arch. Microbiol.* 191, 879–884 (2009).

79 Kiedrowski MR, Kavanaugh JS, Malone CL *et al.* Nuclease modulates biofilm formation in community-associated methicillin-resistant *Staphylococcus aureus*. *PLoS ONE* 6, e26714 (2011).

80 Boles BR, Horswill AR. Agr-mediated dispersal of *Staphylococcus aureus* biofilms. *PLoS Pathog.* 4, e1000052 (2008).